

# An estimate of the deepest branches of the tree of life from ancient vertically-evolving genes

Edmund R. R. Moody<sup>1</sup>, Tara A. Mahendrarajah<sup>2</sup>, Nina Dombrowski<sup>2</sup>, James W. Clark<sup>1</sup>, Celine Petitjean<sup>1</sup>, Pierre Offre<sup>2</sup>, Gergely J. Szöllősi<sup>3,4,5</sup>, Anja Spang<sup>2,6\*</sup>, Tom A. Williams<sup>1\*</sup>

1. School of Biological Sciences, University of Bristol, Bristol BS8 1TH, UK.
2. NIOZ, Royal Netherlands Institute for Sea Research, Department of Marine Microbiology and Biogeochemistry; AB Den Burg, The Netherlands
3. Dept. of Biological Physics, Eötvös Loránd University, 1117 Budapest, Hungary
4. MTA-ELTE “Lendület” Evolutionary Genomics Research Group, 1117 Budapest, Hungary;
5. Institute of Evolution, Centre for Ecological Research, 1121 Budapest, Hungary
6. Department of Cell- and Molecular Biology, Science for Life Laboratory, Uppsala University, SE-75123, Uppsala, Sweden

\*Co-corresponding authors: [tom.a.williams@bristol.ac.uk](mailto:tom.a.williams@bristol.ac.uk), [anja.spang@nioz.nl](mailto:anja.spang@nioz.nl)

## Abstract

Core gene phylogenies provide a window into early evolution, but different gene sets and analytical methods have yielded substantially different views of the tree of life. Trees inferred from a small set of universal core genes have typically supported a long branch separating the archaeal and bacterial domains. By contrast, recent analyses of a broader set of non-ribosomal genes have suggested that Archaea may not be very divergent from Bacteria, and that estimates of inter-domain distance are inflated due to accelerated evolution of ribosomal proteins along the inter-domain branch. Resolving this debate is key to determining the diversity of the archaeal and bacterial domains, the shape of the tree of life, and our understanding of the early course of cellular evolution. Here, we investigate the evolutionary history of the marker genes key to the debate. We show that estimates of a reduced Archaea-Bacteria (AB) branch length result from inter-domain gene transfers and hidden paralogy in the expanded marker gene set, which act to artifactually diminish the genetic distance between the two domains. By contrast, analysis of a broad range of manually curated marker gene datasets from a sample of 700 Archaea and Bacteria reveal that current methods likely underestimate the AB branch length due to substitutional saturation and poor model fit; that the best-performing phylogenetic markers tend to support longer inter-domain branch lengths; and that the AB branch lengths of ribosomal and non-ribosomal marker genes are statistically indistinguishable. A phylogeny of prokaryotes inferred from the 27 highest-ranked marker genes, including ribosomal and non-ribosomal markers, supported a long AB branch, recovered a clade of DPANN at the base of the Archaea, and placed CPR within Bacteria as the sister group to the Chloroflexota.

# Introduction

Much remains unknown about the earliest period of cellular evolution and the deepest divergences in the tree of life. Phylogenies encompassing both Archaea and Bacteria have been inferred from a “universal core” set of 16-56 genes encoding proteins involved in translation and other aspects of the genetic information processing machinery (Ciccarelli et al., 2006; Fournier and Gogarten, 2010; Harris et al., 2003; Hug et al., 2016; Mukherjee et al., 2017; Petitjean et al., 2014; Ramulu et al., 2014; Raymann et al., 2015; Theobald, 2010; Williams et al., 2020). These genes are thought to predominantly evolve vertically and are thus best-suited for reconstructing the tree of life (Ciccarelli et al., 2006; Creevey et al., 2011; Ramulu et al., 2014; Theobald, 2010). In these analyses, the branch separating Archaea from Bacteria (hereafter, the AB branch) is often the longest internal branch in the tree (Cox et al., 2008; Gogarten et al., 1989; Hug et al., 2016; Iwabe et al., 1989; Pühler et al., 1989; Williams et al., 2020). In molecular phylogenetics, branch lengths are usually measured in expected numbers of substitutions per site, with a long branch corresponding to a greater degree of genetic change. Long branches can therefore result from high evolutionary rates, long periods of absolute time, or a combination of the two. If a sufficient number of fossils are available to calibrate them then molecular clock models can, in principle, disentangle the contributions of these effects. However, only very few fossil calibrations (Sugitani et al., 2015) are currently available that are old enough to calibrate early divergences (Betts et al., 2018; Horita and Berndt, 1999; Lepland et al., 2002; van Zuilen et al., 2002), and as a result, the ages and evolutionary rates of the deepest branches of the tree, and estimates of the true biodiversity of the archaeal and bacterial domains, remain highly uncertain.

Recently, Zhu et al. (Zhu et al., 2019) inferred a phylogeny from 381 genes distributed across Archaea and Bacteria using the supertree method ASTRAL (Mirarab et al., 2014). In addition to a large increase in the number of genes compared to other universal marker sets, the functional profile of these markers comprises not only proteins involved in information processing but also proteins affiliated with most other functional COG categories, including metabolic processes (Table S1). The genetic distance (branch length) between the domains (Zhu et al., 2019) was estimated from a concatenation of the same marker genes, resulting in a much shorter AB branch length than observed with the core universal markers (Hug et al., 2016; Williams et al., 2020). These analyses were consistent with the hypothesis (Petitjean et al., 2014; Zhu et al., 2019) that the apparent deep divergence of Archaea and Bacteria might be the result of an accelerated evolutionary rate of genes encoding translational and in particular ribosomal proteins along the AB branch as compared to other genes. Interestingly, the same observation was made previously using a smaller set of 38 non-ribosomal marker proteins (Petitjean et al., 2014), although the difference in AB branch length between ribosomal and non-ribosomal markers in that analysis was reported to be substantially lower (roughly two-fold, compared to roughly ten-fold for the 381 protein set (Petitjean et al., 2014; Zhu et al., 2019).

A higher evolutionary rate of ribosomal genes might result from the accumulation of compensatory substitutions at the interaction surfaces among the protein subunits of the ribosome (Petitjean et al., 2014; Valas and Bourne, 2011), or as a compensatory response to the addition or removal of ribosomal subunits early in evolution (Petitjean et al., 2014).

Alternatively, differences in the inferred AB branch length might result from varying rates or patterns of evolution between the traditional core genes (Spang et al., 2015; Williams et al., 2020) and the expanded set (Zhu et al., 2019). Substitutional saturation (multiple substitutions at the same site (Jeffroy et al., 2006)) and across-site compositional heterogeneity can both impact the inference of tree topologies and branch lengths (Foster, 2004; Lartillot et al., 2007; Lartillot and Philippe, 2004; Quang et al., 2008; Wang et al., 2008). These difficulties are particularly significant for ancient divergences (Gouy et al., 2015). Failure to model site-specific amino acid preferences has previously been shown to lead to under-estimation of the AB branch length due to a failure to detect convergent changes (Tourasse and Gouy, 1999; Williams et al., 2020), although the published analysis of the 381 marker set did not find evidence of a substantial impact of these features on the tree as a whole (Zhu et al., 2019). Those analyses also identified phylogenetic incongruence among the 381 markers, but did not determine the underlying cause (Zhu et al., 2019).

This recent work (Zhu et al., 2019) raises two important issues regarding the inference of the universal tree: first, that estimates of the genetic distance between Archaea and Bacteria from classic “core genes” may not be representative of ancient genomes as a whole, and second, that there may be many more suitable genes to investigate early evolutionary history than generally recognized, providing an opportunity to improve the precision and accuracy of deep phylogenies. Here, we investigate these issues in order to determine why different marker sets support different Archaea-Bacteria branch lengths. First, we examine the evolutionary history of the 381 gene marker set (hereafter, the expanded marker gene set) and identify several features of these genes, including instances of inter-domain gene transfers and mixed paralogy, that may contribute to the inference of a shorter AB branch length in supertree and concatenation analyses. Then, we re-evaluate the marker gene sets used in a range of previous analyses to determine how these and other factors, including substitutional saturation and model fit, contribute to inter-domain branch length estimations and the shape of the universal tree. Finally, we identify a subset of marker genes least affected by these issues, and use these to estimate an updated tree of the primary domains of life and the genetic distance between Archaea and Bacteria.

# Results and Discussion

## Gene transfers and hidden paralogy obscure the genetic distance between Archaea and Bacteria

### ***Genes from the expanded marker set are not widely distributed in Archaea***

The 381 gene set was derived from a larger set of 400 genes used to estimate the phylogenetic placement of new lineages as part of the PhyloPhlAn method (Segata et al., 2013). Perhaps reflecting the focus on bacteria in the original application, the phylogenetic distribution of the 381 marker genes in the expanded set varies substantially (Table S1), with many being poorly represented in Archaea. Indeed 25% of the published gene trees (<https://biocore.github.io/wol/> (Zhu et al., 2019)) contain less than 0.5% archaeal homologues, with 21 (5%) and 69 (18%) of these trees including no or less than 10 archaeal homologues, respectively. For the remaining 75% of the gene trees, archaeal homologs comprise 0.5%-13.4% of the dataset. While there are many more sequenced bacteria than archaea, 63% of the gene trees possessed genes from less than half of the 669 archaeal genomes included in the analysis, whereas only 22% of the gene trees possessed fewer than half of the total number of 9906 sampled bacterial genomes. These distributions suggest that many of these genes are not broadly present in both domains, and that some might be specific to Bacteria.

### ***Conflicting evolutionary histories of individual marker genes and the inferred species tree***

In the focal analysis of the 381 gene set, the tree topology was inferred using the supertree method ASTRAL (Mirarab et al., 2014), with branch lengths inferred on this fixed tree from a marker gene concatenation (Zhu et al., 2019). The topology inferred from this expanded marker set (Zhu et al., 2019) is similar to published trees (Castelle and Banfield, 2018; Hug et al., 2016) and recovers Archaea and Bacteria as reciprocally monophyletic domains, albeit with a shorter AB branch than in earlier analyses. However, the individual gene trees (Zhu et al., 2019) disagree regarding domain monophyly: Archaea and Bacteria are recovered as reciprocally monophyletic groups in only 24 of the 381 published (Zhu et al., 2019) maximum likelihood (ML) gene trees of the expanded marker set (Table S1).

Since single gene trees often fail to strongly resolve ancient relationships, we used approximately-unbiased (AU) tests (Shimodaira, 2002) to evaluate whether the failure to recover domain monophyly in the published ML trees is statistically supported. For computational tractability, we performed these analyses on a 1000-species subsample of the full 10,575-species dataset that was compiled in the original study (Zhu et al., 2019). For 79 of the 381 genes, we could not perform the test because the gene was not found on any of the 74 archaeal genomes present in the 1000-species subsample. For the remaining 302 genes, domain monophyly was rejected ( $p < 0.05$ ) for 232 out of 302 (76.8%) genes. As a comparison, we performed the same test on several smaller marker sets used previously to infer a tree of life (Coleman et al., 2021; Petitjean et al., 2014; Williams et al., 2020); none of

the markers in those sets rejected reciprocal domain monophyly ( $p > 0.05$  for all genes, Figure 1(a)). In what follows, we refer to four published marker gene sets as: the Expanded set (381 genes (Zhu et al., 2019)), the Core set (49 genes (Williams et al., 2020), encoding ribosomal proteins and other conserved information-processing functions; itself a consensus set of several earlier studies (Da Cunha et al., 2017; Spang et al., 2015; Williams et al., 2012)), the Non-ribosomal set (38 genes, broadly distributed and explicitly selected to avoid genes encoding ribosomal proteins (Petitjean et al., 2014)), and the Bacterial set (29 genes used in a recent analysis of bacterial phylogeny (Coleman et al., 2021)).

To investigate why 232 of the marker genes rejected the reciprocal monophyly of Archaea and Bacteria, we returned to the full dataset (Zhu et al., 2019), annotated each sequence in each marker gene family by assigning proteins to KOs, Pfams, and Interpro domains, among others (Table S1, see Methods for details) and manually inspected the tree topologies (Table S1). This revealed that the major cause of domain polyphyly observed in gene trees was inter-domain gene transfer (in 357 out of 381 gene trees (93.7%)) and mixing of sequences from distinct paralogous families (in 246 out of 381 gene trees (64.6%)). For instance, marker genes encoding ABC-type transporters (p0131, p0151, p0159, p0174, p0181, p0287, p0306, p0364), tRNA synthetases (i.e. p0000, p0011, p0020, p0091, p0094, p0202), aminotransferases and dehydratases (i.e. p0073/4-aminobutyrate aminotransferase; p0093/3-isopropylmalate dehydratase) often comprised a mixture of paralogues.

Together, these analyses indicate that the evolutionary histories of the individual markers of the expanded set differ from each other and from the species tree. Zhu et al. acknowledged (Zhu et al., 2019) the varying levels of congruence between the marker phylogenies and the species tree, but did not investigate the underlying causes. Our analyses establish the basis for these disagreements in terms of gene transfers and the mixing of orthologues and paralogues within and between domains. Concatenation is based on the assumption that all of the genes in the supermatrix evolve on the same underlying tree; genes with different gene tree topologies violate this assumption and should not be concatenated because the topological differences among sites are not modelled, and so the impact on inferred branch lengths is difficult to predict. In practice, it is often difficult to be certain that all of the markers in a concatenate share the same gene tree topology, and the analysis proceeds on the hypothesis that a small proportion of discordant genes are not expected to seriously impact the inferred tree. However, the concatenated tree inferred from the expanded marker set differs from previous trees in that the genetic distance between Bacteria and Archaea is greatly reduced, such that the AB branch length appears comparable to distances among bacterial phyla (Zhu et al., 2019). Because an accurate estimate of the AB branch length has a major bearing on unanswered questions regarding the root of the universal tree (Gouy et al., 2015), we next evaluated the impact of the conflicting gene histories within the expanded marker set on inferred AB branch length.

### ***The inferred branch length between Archaea and Bacteria is artifactually shortened by inter-domain gene transfer and hidden paralogy***

To investigate the impact of gene transfers and mixed paralogy on the AB branch length inferred by gene concatenations (Zhu et al., 2019), we compared branch lengths estimated from markers that rejected ( $AU < 0.05$ ) or did not reject ( $AU > 0.05$ ) the reciprocal monophyly of Bacteria and Archaea in the 381 marker set (Figure 1(a)). To estimate AB branch lengths



for genes in which the domains were not monophyletic in the ML tree, we first performed a constrained ML search to find the best gene tree that was consistent with domain monophyly for each family under the LG+G4+F model in IQ-TREE 2 (Minh et al., 2020). While it may seem strained to estimate the length of a branch that does not appear in the ML tree, we reasoned that this approach would provide insight into the contribution of these genes to the AB branch length in the concatenation, in which they conflict with the overall topology. AB branch lengths were significantly ( $P=2.159\times 10^{-12}$ , Wilcoxon rank sum test) shorter for markers that rejected domain monophyly (Figure 1(a);  $<0.05$ : mean AB branch length in expected substitutions/site 0.0130,  $>0.05$ : mean AB branch length 0.559). This result suggests that inter-domain gene transfers reduce the AB branch length when included in a concatenation. This behaviour might result from marker gene transfers reducing the number of fixed differences between the domains, so that the AB branch length in a tree in which Archaea and Bacteria are constrained to be reciprocally monophyletic will tend towards 0 as the number of transfers increases. Consistent with this hypothesis, we observed that  $\Delta LL$ , the difference in log likelihood between the constrained ML tree and ML gene tree (used here as a proxy for gene verticality), correlates negatively with AB branch length (Figure 1(b)). Furthermore, AB branch length decreased as increasing numbers of low-verticality markers were added to the concatenate (Figure 1(c)). Taken together, these results indicate that the inclusion of genes that do not support the reciprocal monophyly of Archaea and Bacteria in the universal concatenate reduces the estimated AB branch length by homogenizing the genetic diversity of the two domains.

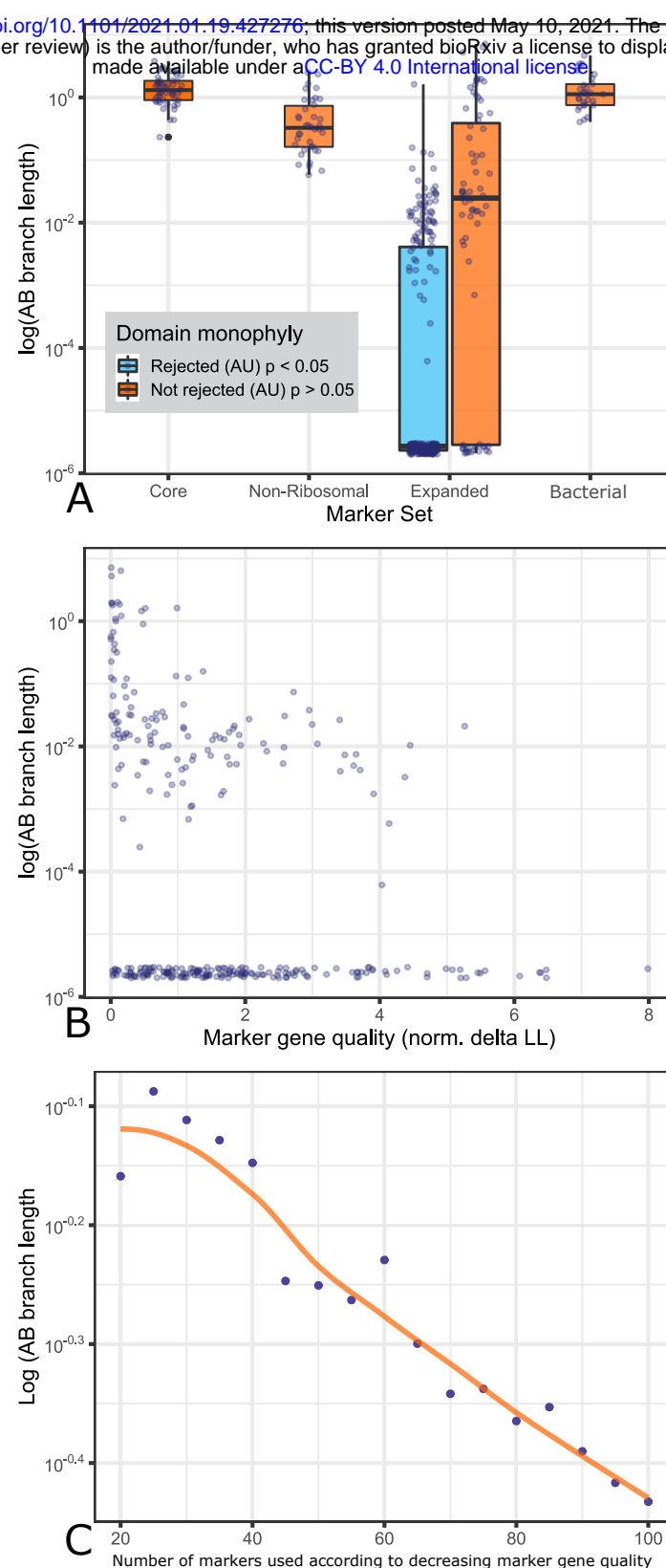


**Figure 1: Expanded set genes in which Archaea and Bacteria are not monophyletic support a shorter AB branch.** (a) Expanded set genes that reject domain monophyly ( $p < 0.05$ , AU test) support significantly shorter AB branch lengths when constrained to follow a domain monophyletic tree ( $p = 2.159 \times 10^{-12}$ , Wilcoxon rank-sum test). None of the marker genes from several other published analyses reject domain monophyly ( $p > 0.05$ , AU test) for all genes tested. (b) Marker gene verticality ( $\Delta LL$ , see below) for the expanded gene set normalized by alignment length correlates negatively with the length of the AB branch between Archaea and Bacteria ( $R^2 = 0.03998$ ,  $p = 0.0004731$ ). (c) Concatenations of 20-100 markers of the expanded set markers ranked by marker gene verticality ( $\Delta LL$ ) show the same trend, with a reduction in AB branch length as markers with a greater  $\Delta LL$  are added to the concatenate.  $\Delta LL$  is the difference between the log likelihood of the ML gene family tree under a free topology search and the log likelihood of the best tree constrained to obey domain monophyly. The trendline is estimated using LOESS regression.

# ***The age of the last universal common ancestor (LUCA) inferred from strict clocks does not predict marker gene quality***

Reliable age estimates using molecular clock methods require calibrations, but few calibrations exist for the deeper branches of the tree of life. Zhu et al. (Zhu et al., 2019) argued that the expanded marker set is useful for deep phylogeny because estimates of the age of the last universal common ancestor (LUCA) obtained by fitting molecular clocks to their dataset are in agreement with the geological record: a root (LUCA) age of 3.6-4.2 Ga was inferred from the entire 381-gene dataset, consistent with the earliest fossil evidence for life (Betts et al., 2018; Sugitani et al., 2015), whereas estimates from ribosomal markers alone supported a root age of 7 Ga. This age might be considered implausible because it is much older than the age of the Earth and Solar System (with the moon-forming impact occurring ~4.51 Ga (Barboni et al., 2017; Hanan and Tilton, 1987)). However, the palaeobiological plausibility of the age estimate from the 381 gene set does not, in itself, constitute evidence of marker gene suitability. In the original analyses, the age of LUCA was estimated using a maximum likelihood approach, as well as a Bayesian molecular clock with a strict clock (assuming a constant evolutionary rate) or a relaxed clock with a single calibration. A strict clock model does not permit changes in evolutionary rate through time or across branches, and so a longer AB branch will lead to an older inferred LUCA age. Likewise, a relaxed clock model with a single calibration may fail to distinguish molecular distances and geological time. Given that the short AB branch in the expanded gene set results, in part, from phylogenetic incongruence among markers, we evaluated the age of LUCA inferred from the subset of the expanded gene set least affected by these issues. To do so, we analysed the top 5% of gene families according to their  $\Delta$ LL score (a set of 20 genes, which includes only 1 ribosomal protein) under the same clock model parameters as the original dataset (Figure 2). This analysis resulted in a significantly more ancient age estimate for LUCA (5.5-6.5 Ga), and trimming the alignment to remove poorly-aligning regions resulted in a still older estimate (6.34-6.89 Ga), approaching that of the ribosomal genes (7.46-8.03 Ga). These analyses suggest that, for these data and calibrations, the inferred age for LUCA is not a reliable indicator of marker quality, because analyses using the subset of the data least affected by incongruence more clearly reveals the underlying limitations of strict clock analyses (and indeed relaxed clocks with few calibrations) for dating ancient divergences. In principle, more reliable estimates of LUCA's age might be obtained by using more calibrations. However, unambiguous calibrations remain elusive, particularly for the root and other deep branches of the tree. Despite advances in molecular clock methodology, such calibrations represent the only way to reliably capture the relationship between genetic distance and divergence time.



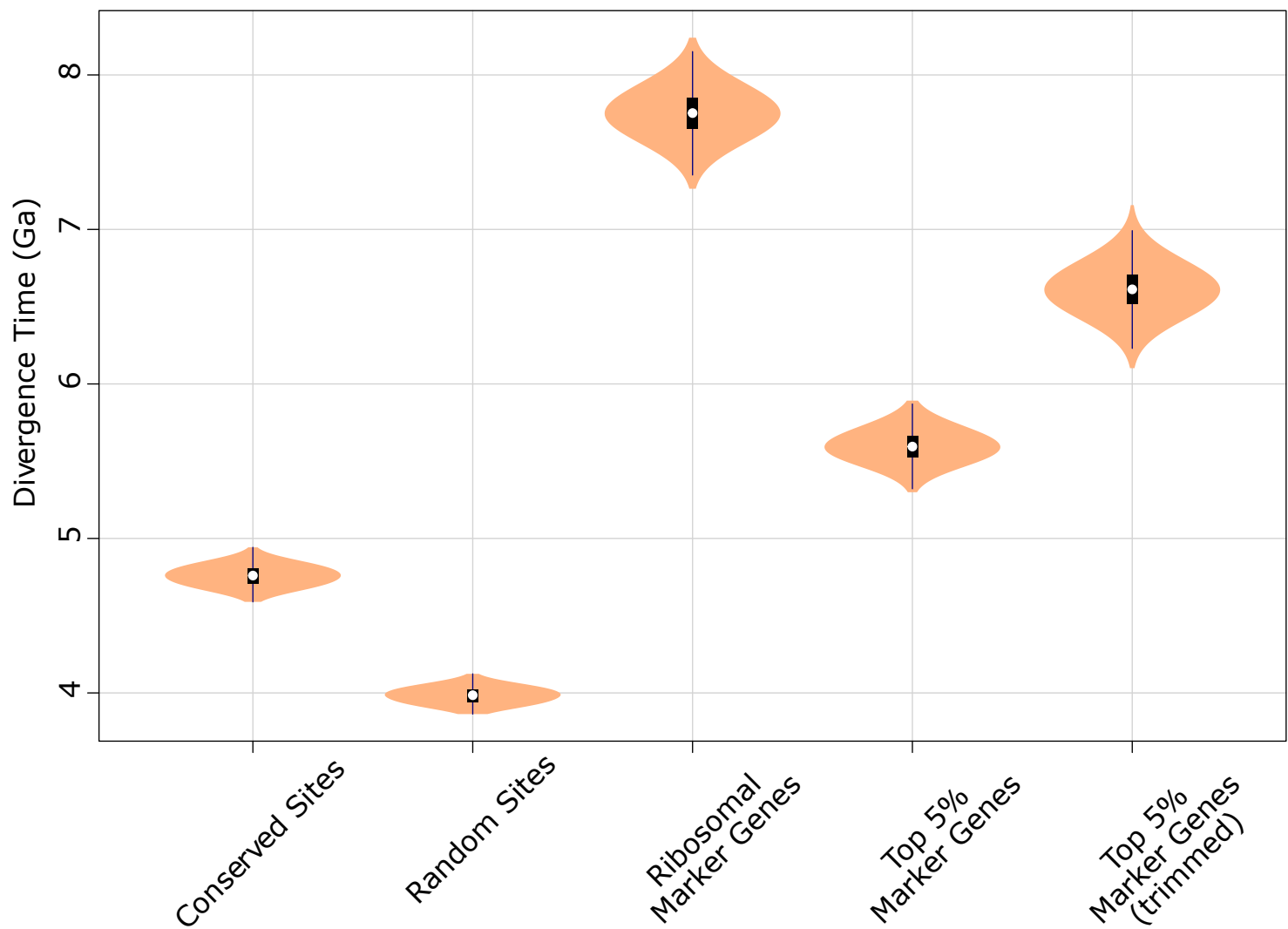


**Figure 2. The inferred age of LUCA is not a reliable indicator of marker quality.** Posterior node age estimates from Bayesian molecular clock analyses of 1) Conserved sites as estimated previously (Zhu et al., 2019); 2) Random sites (Zhu et al., 2019) 3) Ribosomal genes (Zhu et al., 2019) 4) The top 5% of marker gene families according to their  $\Delta$ LL score (including only 1 ribosomal protein) and 5) The same top 5% of marker genes trimmed using BMGE(Crisciuolo and Gribaldo, 2010) to remove highly variable sites. In each case, a strict molecular clock was applied, with the age of the Cyanobacteria-Melainabacteria split constrained between 2.5 and 2.6 Ga.

# Phylogeny of Archaea and Bacteria using ancient vertically-evolving genes

## *Finding ancient vertically-evolving genes*

To estimate the AB branch length and the phylogeny of prokaryotes using a dataset that resolves some of the issues identified above, we performed a meta-analysis of several previous studies to identify a consensus set of vertically-evolving marker genes. We identified unique markers from these analyses by reference to the COG ontology (Dombrowski et al., 2020; Galperin et al., 2019), extracted homologous sequences from a representative sample of 350 archaeal and 350 bacterial genomes, and performed iterative phylogenetics and manual curation to obtain a set of 54 markers that recovered archaeal and bacterial monophyly (see Methods). Subsequently, we ranked these 54 genes by the extent to which they recovered established within-domain relationships using the split score, a criterion described previously (Dombrowski et al., 2020) (see Methods) yielding a final set of 27 markers that were used for inferring an updated universal species tree (see below). Marker genes that better resolved relationships within each domain also supported a longer AB branch length (Figure 3).

## *Distributions of AB branch lengths for ribosomal and non-ribosomal marker genes are similar*

Traditional universal marker sets include many ribosomal proteins (Ciccarelli et al., 2006; Fournier and Gogarten, 2010; Harris et al., 2003; Hug et al., 2016; Williams et al., 2020). If ribosomal proteins experienced accelerated evolution during the divergence of Archaea and Bacteria, this might lead to the inference of an artifactually long AB branch length (Petitjean et al., 2014; Zhu et al., 2019). To investigate this, we plotted the inter-domain branch lengths for the 38 and 16 ribosomal and non-ribosomal genes, respectively, comprising the 54 marker genes set. We found no evidence that there was a longer AB branch associated with ribosomal markers (Figure 4; mean AB branch length for ribosomal proteins 1.35, mean for non-ribosomal 2.25). Prior to manual curation, non-ribosomal markers had a greater number of HGTs and cases of mixed paralogy. In particular, for the original set of 95 markers, 62% of the non-ribosomal markers and 21% of the ribosomal markers were not monophyletic, respectively. These values were 69% and 29% for the 54 markers, and 50% and 33% for the 27 markers. These results imply that manual curation of marker genes is important for deep phylogenetic analyses, particularly when using non-ribosomal markers.

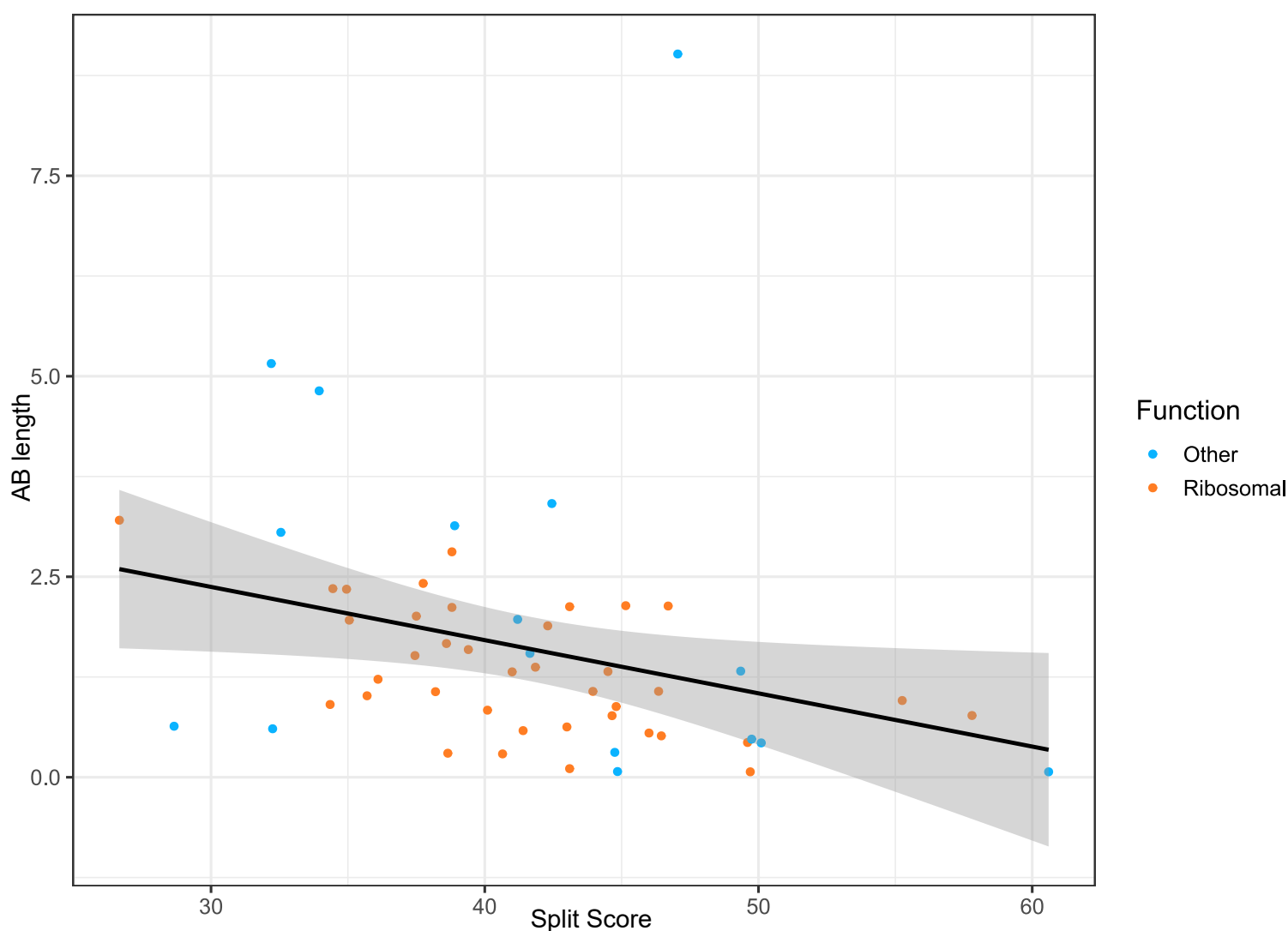


**Figure 3. Better phylogenetic markers have longer AB branches.** The plot shows the relationship between split score (a lower split score denotes better recovery of established within-domain relationships, see Methods) and AB branch length (in expected number of substitutions/site) for the 54 highest-ranked marker genes. Marker genes with higher split scores (that split monophyletic groups into multiple subclades) have shorter AB branch lengths ( $P = 0.0311$ ,  $r = 0.294$ ). Split scores of ribosomal and non-ribosomal markers were statistically indistinguishable ( $P = 0.828$ , Figure S3).

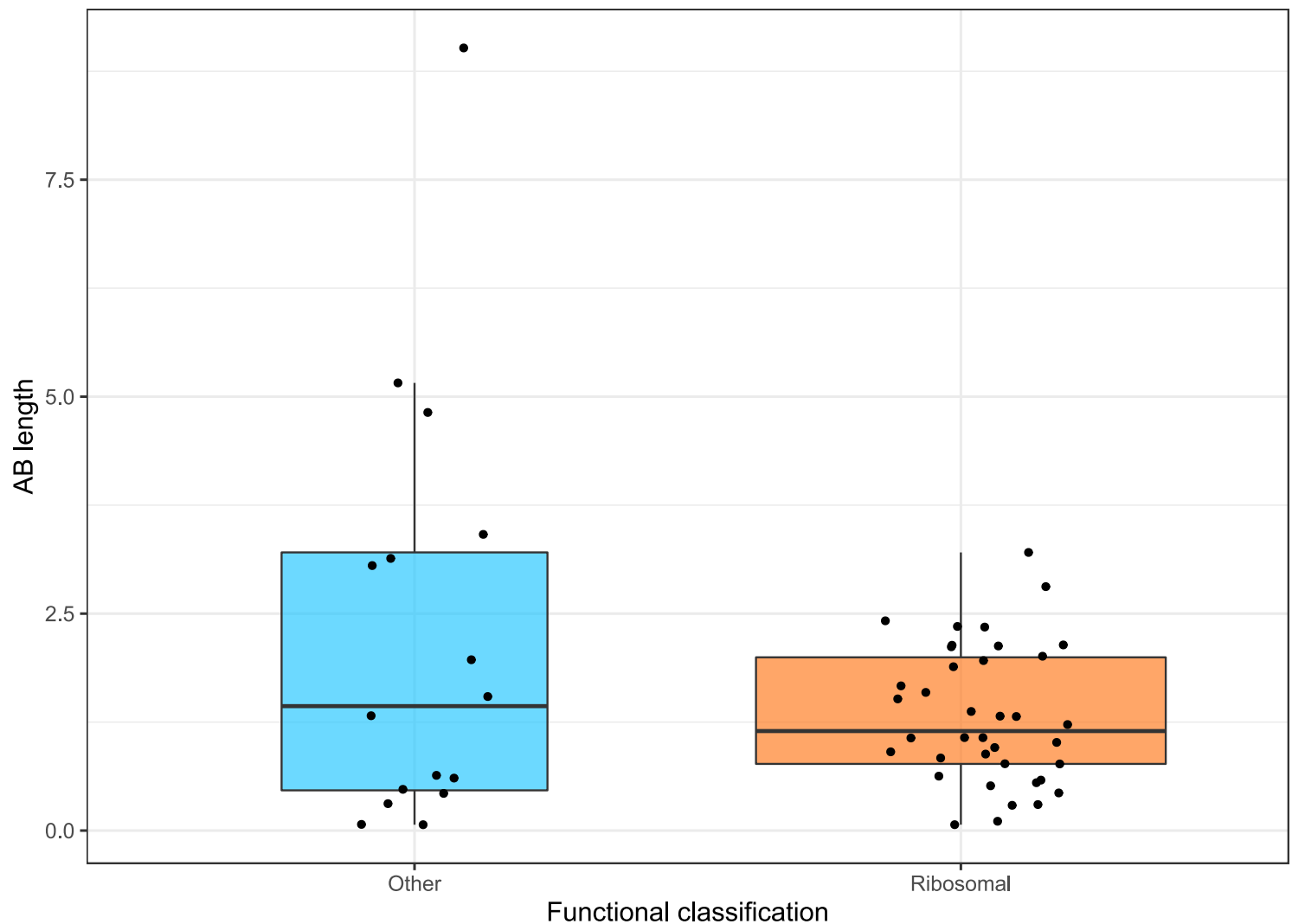


**Figure 4. Among vertically-evolving marker genes, ribosomal genes do not have a longer AB branch length.** The plot shows functional classification of markers against AB branch length using the 54 most vertically evolving markers. We did not see a significant ( $P = 0.619$ , Wilcoxon rank sum test) difference between AB branch lengths for ribosomal and non-ribosomal genes.

# ***Substitutional saturation and poor model fit contribute to underestimation of AB branch length***

For the top 50% of marker genes as determined by split scores (27 genes), we performed an additional round of single gene tree inference and manual review to identify and remove remaining sequences which had evidence of HGT or represented distant paralogs. The resulting single gene trees are provided in the Data Supplement (10.6084/m9.figshare.13395470). To evaluate the relationship between site evolutionary rate and AB branch length, we created two concatenations: fastest sites (comprising sites with highest probability of being in the fastest Gamma rate category; 868 sites) and slowest sites (sites with highest probability of being in the slowest Gamma rate category, 1604 sites) and compared relative branch lengths inferred from the entire concatenate using IQ-TREE 2 to infer site-specific rates (Figure 5). As expected, total tree length is shorter from the slow-evolving sites, but the relative AB branch length is longer (1.2 substitutions/site, or ~2% of total tree length, compared to 2.6 substitutions/site, or ~0.04% total tree length for the fastest-evolving sites). This result suggests that, at fast-evolving sites, some changes along the AB branch have been overwritten by later events in evolution --- that is, that substitutional saturation leads to an underestimate of the AB branch length.

Another factor that has been shown to lead to underestimation of genetic distance on deep branches is a failure to adequately model the site-specific features of sequence evolution (Lartillot and Philippe, 2004; Schrempf et al., 2020; Wang et al., 2018; Williams et al., 2020). Amino acid preferences vary across the sites of a sequence alignment, due to variation in the underlying functional constraints (Lartillot and Philippe, 2004; Quang et al., 2008; Wang et al., 2008). The consequence is that, at many alignment sites, only a subset of the twenty possible amino acids are tolerated by selection. Standard substitution models, such as LG+G4+F, are site-homogeneous, and approximate the composition of all sites using the average composition across the entire alignment. Such models underestimate the rate of evolution at highly constrained sites because they do not account for the high number of multiple substitutions that occur at such sites. The effect is that site-homogeneous models underestimate branch lengths when fit to site-heterogeneous data. Site-heterogeneous models have been developed that account for site-specific amino acid preferences, and these generally show improved fit to real protein sequence data (reviewed in (Williams et al., 2021)). To evaluate the impact of substitution model fit for these data, we fit a range of models to the full concatenation, assessing model fit using the Bayesian information criterion (BIC) in IQ-TREE 2. The AB branch length inferred under the best-fit model, the site-heterogeneous LG+C60+G4+F model, was 2.52 substitutions/site, ~1.7-fold greater than the branch length inferred from the site-homogeneous LG+G4+F model (1.45 substitutions/site). Thus, substitution model fit has a major effect on the estimated length of the AB branch, with better-fitting models supporting a longer branch length (Table 1). The same trends are evident when better-fitting site-heterogeneous models are used to analyse the dataset of Zhu et al.: considering only the top 5% of genes by  $\Delta$ LL score, the AB branch length is 1.2 under LG+G4+F, but increases to 2.4 under the best-fitting LG+C60+G4+F model (Figure S2).

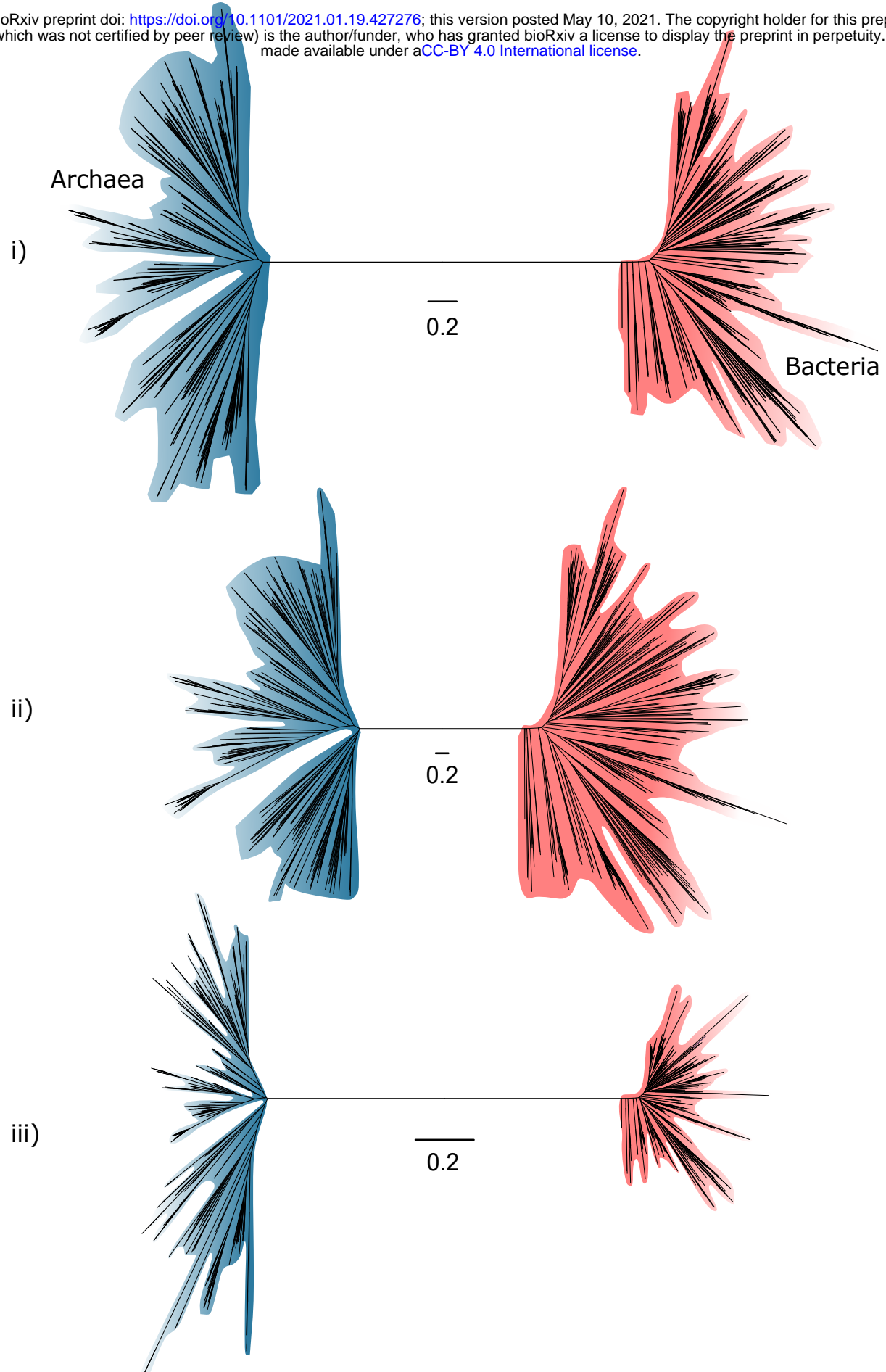


**Figure 5. Slow- and fast-evolving sites support different shapes for the universal tree.** (i) Tree of Archaea and Bacteria inferred from a concatenation of 27 core genes; (ii) Tree inferred from the fastest-evolving sites; (iii) Tree inferred from the slowest-evolving sites. To facilitate comparison of relative diversity, scale bars are provided separately for each panel. Slow-evolving sites support a relatively long inter-domain branch and less diversity within the domains (that is, shorter between-taxa branch lengths within domains). This suggests that substitution saturation (overwriting of earlier changes) may reduce the relative length of the AB branch at fast-evolving sites and genes.



Substitution model	BIC	AB branch length
LG+G4+F	5935950.053	1.449090256
LG+C20+G4+F	5783903.997	2.139350118
LG+C40+G4+F	5756823.360	2.469702112
LG+C60+G4+F	5746886.292	2.517828771

**Table 1. The inferred AB length from a concatenation of the top 27 markers using a simple model versus models which account for site compositional heterogeneity.** Using better fitting models, i.e models which allow for across-site compositional heterogeneity, a longer AB branch is inferred.

### ***A phylogeny of Archaea and Bacteria inferred from 27 vertically-evolving marker genes***

The topology of our phylogeny of the primary domains of life (Figure 6) is consistent with recent single-domain trees inferred for Archaea and Bacteria independently (Coleman et al., 2021; Dombrowski et al., 2020; Williams et al., 2017), although the deep relationships within Bacteria are only poorly resolved, with the exception of the monophyly of Gracilicutes (Figure 6). A recent analysis suggested that, among extant lineages, the metabolisms of Clostridia, Deltaproteobacteria, Actinobacteria and some Aquificae might best preserve the metabolism of the last bacterial common ancestor (Xavier et al., 2021). Assuming a universal root between Archaea and Bacteria (Dagan et al., 2010; Gogarten et al., 1989; Iwabe et al., 1989), none of these groups branch near the bacterial root in our analysis (Figure 6). This is consistent with previous work (Castelle and Banfield, 2018; Hug et al., 2016; Parks et al., 2017; Raymann et al., 2015) including the inference of an updated and rooted bacteria phylogeny (Coleman et al., 2021). Notably, our analysis placed the Candidate Radiation (CPR) (Brown et al., 2015) as a sister lineage to Chloroflexi (Chloroflexota) rather than as a deep-branching bacterial superphylum. While this contrasts with initial trees suggesting that CPR may represent an early diverging sister lineage of all other Bacteria (Brown et al., 2015; Castelle and Banfield, 2018; Hug et al., 2016), our finding is consistent with recent analyses that recovered CPR within the Terrabacteria (Coleman et al., 2021; Taib et al., 2020). Together, these analyses suggest that the deep-branching position of CPR in some trees was a result of long branch attraction, a possibility that has been raised previously (Hug et al., 2016; Méheust et al., 2019).

The deep branches of the archaeal subtree are well-resolved in the ML tree and recover clades of DPANN (albeit at 51% bootstrap support), Asgard (100% bootstrap support), and TACK Archaea (75% bootstrap support), in agreement with a range of previous studies (Dombrowski et al., 2020; Guy and Ettema, 2011; Raymann et al., 2015; Williams et al., 2017). We also find support for the placement of Methanonatronarchaeia (Sorokin et al., 2017) distant to Halobacteria within the Methanotecta, in agreement with recent analyses and suggesting their initial placement with Halobacteria (Sorokin et al., 2017) may be an artifact of compositional attraction (Aouad et al., 2019; Dombrowski et al., 2020; Martijn et al., 2020). Notably, the Hadesarchaea (92% bootstrap support) and a clade comprising Theionarchaea, Methanofastidiosa, and Thermococcales (92% bootstrap support) branch basal to the TACK

and Asgard Archaea, respectively, in our analysis, rather than with other Euryarchaeota. These positions have been previously reported (Adam et al., 2017; Raymann et al., 2015; Williams et al., 2017), though the extent of euryarchaeotal paraphyly and the lineages involved has varied among analyses.

A broader observation from our analysis is that the phylogenetic diversity of the archaeal and bacterial domains, measured as substitutions per site in this consensus set of vertically-evolving marker genes, appears to be similar (Figure 5(i); the mean root to tip distance for archaea: 2.38, for bacteria: 2.41, the range of root to tip distances for archaea: 1.79-3.01, for bacteria: 1.70-3.17). Considering only the slowest-evolving category of sites, branch lengths within Archaea are actually longer than within Bacteria (Figure 5(iii)). This result differs from some published trees (Hug et al., 2016; Zhu et al., 2019) in which the phylogenetic diversity of Bacteria has appeared to be significantly greater than that of Archaea. By contrast to those earlier studies, we analysed a set of 350 genomes from each domain, an approach which may tend to reduce the differences between them. While we had to significantly downsample the sequenced diversity of Bacteria, our sampling nonetheless included representatives from all known major lineages of both domains, and so might be expected to recover a difference in diversity, if present. Our analyses and a number of previous studies (Hug et al., 2016; Parks et al., 2018; Petitjean et al., 2014; Zhu et al., 2019) indicate that the choice of marker genes has a profound impact on the apparent phylogenetic diversity of prokaryotic groups; for instance, in the proportion of bacterial diversity composed of CPR (Hug et al., 2016; Parks et al., 2017). Our results demonstrate that slow and fast-evolving sites from the same set of marker genes support different tree shapes and branch lengths; it therefore seems possible that between-dataset differences are due, at least in part, to evolutionary rate variation within and between marker genes.

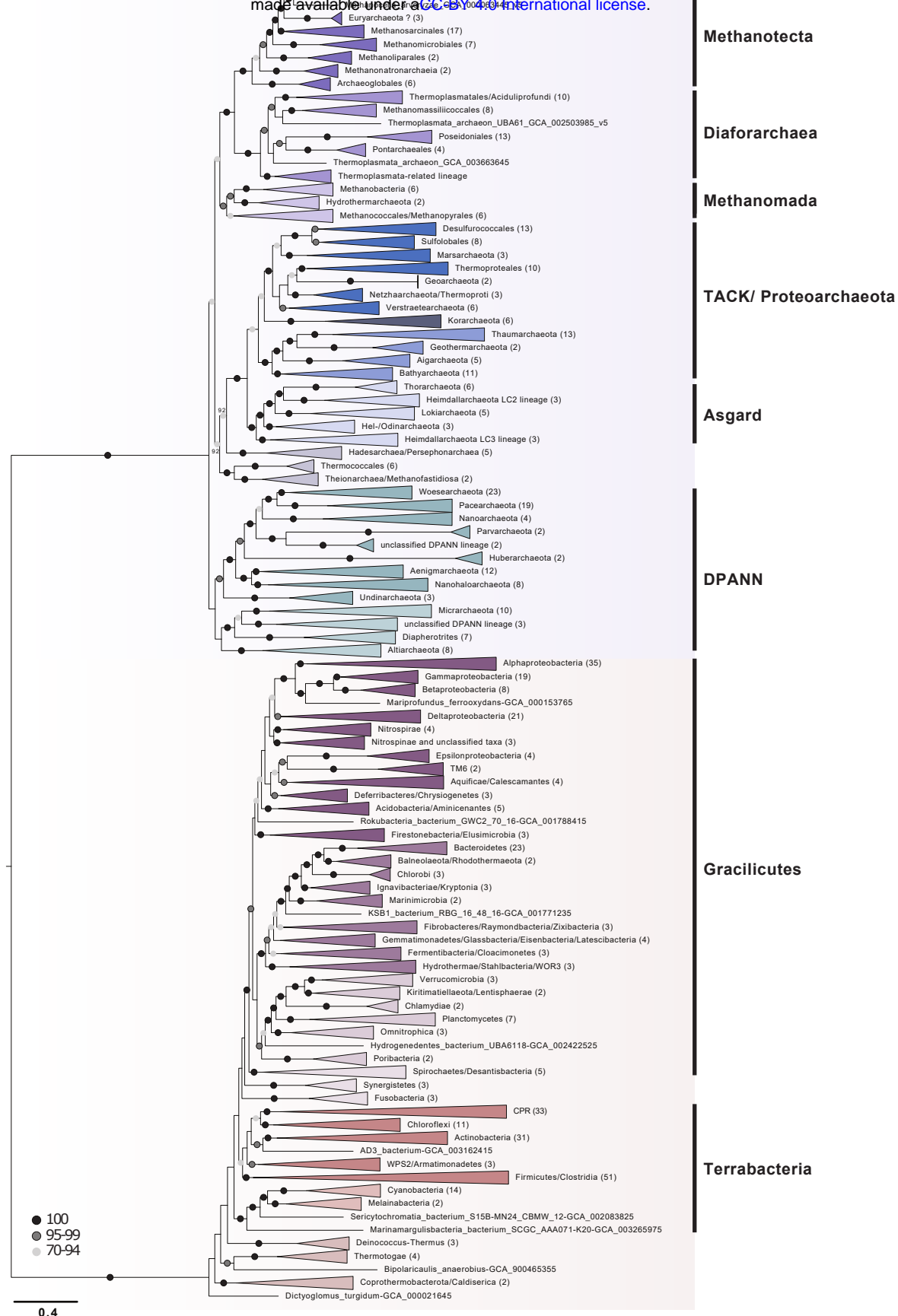


**Figure 6: A phylogeny of Archaea and Bacteria inferred from a concatenation of 27 marker genes.** Consistent with some recent studies (Dombrowski et al., 2020; Guy and Ettema, 2011; Raymann et al., 2015; Williams et al., 2017), we recovered the DPANN, TACK and Asgard Archaea as monophyletic groups. Although the deep branches within Bacteria are poorly resolved, we recovered a sister group relationship between CPR and Chloroflexota, consistent with a recent report (Coleman et al., 2021). The tree was inferred using the best-fitting LG+C60+G4+F model in IQ-TREE 2 (Minh et al., 2020). Branch lengths are proportional to the expected number of substitutions per site. Support values are ultrafast (UFBoot2) bootstraps (Hoang et al., 2018). Numbers in parenthesis refer to number of taxa within each collapsed clade. Please note that collapsed taxa in the Archaea and Bacteria roughly correspond to order- and phylum-level lineages, respectively.

## Conclusion

Core gene phylogenies provide a window into the earliest period of archaeal and bacterial evolution. Concatenation is useful for pooling signal across individual genes, but topology and branch length estimates from concatenations only reflect the underlying tree of life if the individual genes share the same evolutionary history. Our analysis of published datasets (Coleman et al., 2021; Petitjean et al., 2014; Williams et al., 2020; Zhu et al., 2019) indicates that incongruence among marker genes resulting from inter-domain gene transfer and hidden paralogy can lead to an under-estimate of the inter-domain branch length. We performed a re-analysis of marker genes from a range of published analyses, manually curated datasets to identify and remove transferred genes, and estimated an updated phylogeny of Archaea and Bacteria. Considering only this manually curated consensus marker gene dataset, we found no evidence that ribosomal markers overestimate stem length; since they appear to be transferred less frequently than other genes, our analysis affirms that ribosomal proteins are useful markers for deep phylogeny. In general, better markers, regardless of functional category, support a longer AB branch length. A phylogeny inferred from the 27 best-performing markers was consistent with some recent work on early prokaryotic evolution, resolving the major clades within Archaea and nesting the CPR within Terrabacteria. Our analyses suggest that both the true Archaea-Bacteria branch length (Figure 7), and the phylogenetic diversity of Archaea, may be underestimated by even the best current models, a finding that is consistent with a root for the tree of life between the two prokaryotic domains.

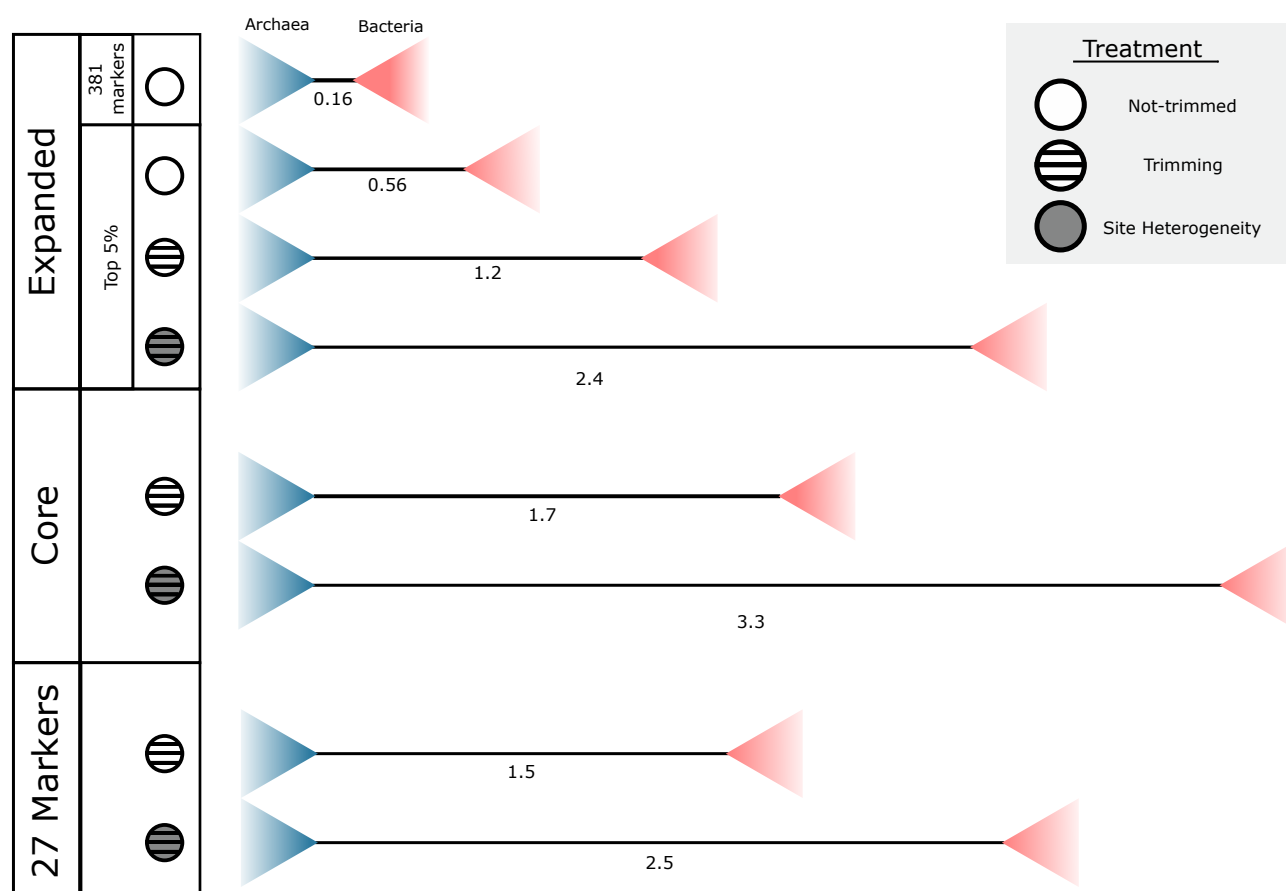


**Figure 7. The impact of marker gene choice, phylogenetic congruence, alignment trimming, and substitution model fit on estimates of the Archaea-Bacteria branch length.** Analysis using a site-homogeneous model (LG+G4+F) on the complete 381-gene expanded set results in an AB branch substantially shorter than previous estimates. Removing the genes most seriously affected by inter-domain gene transfer, trimming poorly-aligned sites using BMGE (Criscuolo and Gribaldo, 2010), and using the best-fitting site-heterogeneous model available (LG+C60+G4+F) substantially increase the estimated AB length, such that it is comparable with published estimates from the “core” set (Williams et al., 2020) and the consensus set of 27 markers identified in the present study. Branch lengths measured in expected number of substitutions/site.

# Methods

## Data

We downloaded the individual alignments from (Zhu et al., 2019) (<https://github.com/biocore/wol/tree/master/data/>), along with the genome metadata and the individual newick files. We checked each published tree for domain monophyly, and also performed approximately unbiased (AU) (Shimodaira, 2002) tests to assess support for domain monophyly on the underlying sequence alignments using IQ-TREE 2 (Minh et al., 2020). The phylogenetic analyses were carried out using the ‘reduced’ subset of 1000 taxa outlined by the authors (Zhu et al., 2019), for computational tractability. These markers were also trimmed according to the protocol in the original paper (Zhu et al., 2019), i.e sites with >90% gaps were removed, followed by removal of sequences with >66% gaps.

We also downloaded the Williams et al. (Williams et al., 2020) (“core”), Petitjean et al. (Petitjean et al., 2014) (“non-ribosomal”) and Coleman et al. (Coleman et al., 2021) (“bacterial”) datasets from their original publications.

## Annotations

Proteins used for phylogenetic analyses by Zhu *et al.* (Zhu et al., 2019), were annotated to investigate the selection of sequences comprising each of the marker gene families. To this end, we downloaded the protein sequences provided by the authors from the following repository: <https://github.com/biocore/wol/tree/master/data/alignments/genes>. To obtain reliable annotations, we analysed all sequences per gene family using several published databases, including the arCOGs (version from 2014) (Seemann, 2014), KOs from the KEGG Automatic Annotation Server (KAAS; downloaded April 2019) (Aramaki et al., 2020), the Pfam database (Release 31.0)(Bateman et al., 2004), the TIGRFAM database (Release 15.0) (Haft et al., 2003), the Carbohydrate-Active enZymes (CAZy) database (downloaded from dbCAN2 in September 2019)(Cantarel et al., 2009), the MEROPs database (Release 12.0) (Rawlings et al., 2016), (Saier et al., 2006), the hydrogenase database (HydDB; downloaded in November 2018) (Søndergaard et al., 2016), the NCBI- non-redundant (nr) database (downloaded in November 2018), and the NCBI COGs database (version from 2020). Additionally, all proteins were scanned for protein domains using InterProScan (v5.29-68.0; settings: --iplookup --goterms) (Jones et al., 2014).

Individual database searches were conducted as follows: arCOGs were assigned using PSI-BLAST v2.7.1+ (settings: -evaluate 1e-4 -show\_gis -outfmt 6 -max\_target\_seqs 1000 -dbsize 100000000 -comp\_based\_stats F -seg no) (Altschul et al., 1997). KOs (settings: -E 1e-5), PFAMs (settings: -E 1e-10), TIGRFAMs (settings: -E 1e-20) and CAZymes (settings: -E 1e-20) were identified in all archaeal genomes using hmmsearch v3.1b2(Finn et al., 2011). The MEROPs and HydDB databases were searched using BLASTp v2.7.1 (settings: -outfmt 6, -evaluate 1e-20). Protein sequences were searched against the NCBI\_nr database using DIAMOND v0.9.22.123 (settings: --more-sensitive --e-value 1e-5 --seq 100 --no-self-hits --taxonmap prot.accession2taxid.gz) (Buchfink et al., 2015). For all database searches the best hit for each protein was selected based on the highest e-value and bitscore and all results are summarized in the Data Supplement Table, Annotation\_Tables/0\_Annotation\_tables\_full/All\_Zhu\_marker\_annotations\_16-12-



2020.tsv.zip. For InterProScan we report multiple hits corresponding to the individual domains of a protein using a custom script (parse\_IPRdomains\_vs2\_GO\_2.py).

Assigned sequence annotations were summarized and all distinct KOs and Pfams were collected and counted for each marker gene. KOs and Pfams with their corresponding descriptions were mapped to the marker gene file downloaded from the repository: <https://github.com/biocore/wol/blob/master/data/markers/metadata.xlsx> and used in summarization of the 381 marker gene protein trees (Table S1).

For manual inspection of single marker gene trees, KO and Pfam annotations were mapped to the tips of the published marker protein trees, downloaded from the repository: <https://github.com/biocore/wol/tree/master/data/trees/genes>. Briefly, the Genome ID, Pfam, Pfam description, KO, KO description, and NCBI Taxonomy string were collected from each marker gene annotation table and were used to generate mapping files unique to each marker gene phylogeny, which links the Genome ID to the annotation information (GenomeID|Domain|Pfam|Pfam Description|KO|KO Description). An in-house perl script `replace_tree_names.pl` ([https://github.com/ndombrowski/Phylogeny\\_tutorial/tree/main/Input\\_files/5\\_required\\_Scripts](https://github.com/ndombrowski/Phylogeny_tutorial/tree/main/Input_files/5_required_Scripts)) was used to append the summarized protein annotations to the corresponding tips in each marker gene tree. Annotated marker gene phylogenies were manually inspected using the following criteria including: 1) retention of reciprocal domain monophyly (Archaea and Bacteria) and 2) for the presence or absence of potential paralogous families. Paralogous groups and misannotated families present in the gene trees were highlighted and violations of search criteria were recorded in Table S1.

## ***Phylogenetic analyses***

### *COG assignment for the Core, Non-Ribosomal, and Bacterial marker genes*

First, all gene sequences in the three published marker sets (core, non-ribosomal, and bacterial) were annotated using the NCBI COGs database (version from 2020). Sequences were assigned a COG family using `hmmsearch` v3.3.2 (Finn et al., 2011) (settings: -E 1e-5) and the best hit for each protein sequence was selected based on the highest e-value and bit score. To assign the appropriate COG family for each marker gene, we quantified the percentage distribution of all unique COGs per gene, and selected the family representing the majority of sequences in each marker gene.

Accounting for overlap, this resulted in 95 unique COG families from the original 119 total marker genes across all three published datasets (Table S2). Orthologues corresponding to these 95 COG families were identified in the 700 genomes (350 Archaea, 350 Bacteria, Table S3) using `hmmsearch` v3.3.2 (settings: -E 1e-5). The reported BinID and protein accession were used to extract the sequences from the 700 genomes, which were used for subsequent phylogenetic analyses.

### *Marker gene inspection and analysis*

We aligned these 95 sequence sets using MAFFT-linsi (Katoh and Toh, 2008) and removed poorly-aligned positions with BMGE (Criscuolo and Gribaldo, 2010). We inferred initial maximum likelihood trees (LG+G4+F) for all 95 markers and mapped the KO and Pfam

domains and descriptions, inferred from annotation of the 700 genomes, to the corresponding tips (see above). Manual inspection took into consideration monophyly of Archaea and Bacteria and the presence of paralogs, and other signs of contamination (HGT, LBA). Accordingly, single gene trees that failed to meet reciprocal domain monophyly were excluded, and any instances of HGT, paralogous sequences, and LBA artefacts were manually removed from the remaining trees resulting in 54 markers across the three published datasets that were subject to subsequent phylogenetic analysis (LG+C20+G4+F) and further refinement (see below).

### *Ranking markers based on split score*

We applied an automated marker gene ranking procedure devised previously, the split score (Dombrowski et al., 2020), to rank each of the 54 markers that satisfied reciprocal monophyly based on the extent to which they recovered established phylum-, class- or, order-level relationships within the archaeal and bacterial domains (Table S4).

The script quantifies the number of splits, or occurrences where a taxon fails to cluster within its expected taxonomic lineage, across all gene phylogenies. Monophyly of archaeal and bacterial lineages was assessed based on clades defined in Table S4. Briefly, we used Cluster1 for Archaea in combination with Cluster0 (phylum) or Cluster3 (i.e. on class-level if defined and otherwise on phylum-level; Table S4) for Bacteria. We then ranked the marker genes using the following split-score criteria: the number of splits per taxon and the splits normalized to the species count. The percentage of split phylogenetic groups was used to determine the highest ranking (top 50%) markers.

### *Concatenation*

Based on the split score ranking of the 54 marker genes (above), the top 50% (27 markers, Table S4) marker genes were manually inspected using criteria as defined above, and contaminating sequences were manually removed from the individual sequence files. Following inspection, marker protein sequences were aligned using MAFFT-LINSI (Katoh and Standley, 2013) and trimmed using BMGE (Criscuolo and Gribaldo, 2010). We concatenated the 27 markers into a supermatrix, which was used to infer a maximum-likelihood tree (Figure 6, under LG+C60+G4+F), evolutionary rates (see below), and rate-category supermatrices as well as to perform model performance tests (see below).

### *Constraint analysis*

We performed a maximum likelihood free topology search using IQ-TREE 2 (Minh et al., 2020) under the LG+G4+F model, with 1000 bootstrap replicates on each of the markers from the expanded, bacterial, core and non-ribosomal sets. We also performed a constrained analysis with the same model, in order to find the maximum likelihood tree in which Archaea and Bacteria were reciprocally monophyletic. We then compared both trees using the approximately unbiased (AU) Shimodaira (2002) test in IQ-TREE 2 (Minh et al., 2020) with 10,000 RELL (Shimodaira, 2002) bootstrap replicates. To evaluate the relationship between marker gene verticality and AB branch length, we calculated the difference in log-likelihood between the constrained and unconstrained trees in order to rank the genes from the expanded marker set, made concatenates comprised of the top 20-100 (intervals of 5) of these

marker genes, and inferred the tree length under LG+C10+G4+F with 1000 bootstrap replicates.

# *Site and gene evolutionary rates*

We inferred rates using the --rate option in IQ-TREE 2 (Minh et al., 2020) for both the 381 marker concatenation from Zhu (Zhu et al., 2019) and the top 5% of marker genes based on the results of difference in log-likelihood between the constrained tree and free-tree search in the constraint analysis (above). We also used this method to explore the differences in rates for the 27 marker set. We built concatenates for sites in the slowest and fastest rate categories, and inferred branch lengths from each of these concatenates using the tree inferred from the corresponding dataset as a fixed topology.

# *Substitution model fit*

Model fit tests were undertaken using the top 5% concatenate described above, with the alignment being trimmed with BMGE 1.12 (Criscuolo and Gribaldo, 2010) with default settings (BLOSUM62, entropy 0.5) for all of the analyses except the 'untrimmed' LG+G4+F run, other models on the trimmed alignment were LG+G4+F, LG+R4+F and LG+C10,20,30,40,50,60+G4+F, with 1000 bootstrap replicates. Model fitting was done using ModelFinder (Kalyaanamoorthy et al., 2017) in IQ-TREE 2 (Minh et al., 2020). For the model testing for the 27 concatenation, we performed a model finder analysis (-m MFP) including additional complex models of evolution, (i.e. LG+C60+G4+F, LG+C50+G4+F, LG+C40+G4+F, LG+C30+G4+F, LG+C20+G4+F, LG+C10+G4+F, LG+G4+F, LG+R4+F) to the default, to find the best fitting model for the analysis. This revealed that, according to AIC, BIC and cAIC, LG+C60+G4+F was the best fitting model. For comparison, we also performed analyses using the following models: LG+G4+F, LG+C20+G4+F, LG+C40+G4+F (Table 1).

# *Molecular clock analyses*

Molecular clock analyses were devised to test the effect of genetic distance on the inferred age of LUCA. Following the approach of Zhu et al (Zhu et al., 2019), we subsampled the alignment to 100 species. Five alternative alignments were analysed, representing conserved sites across the entire alignment, randomly selected sites across the entire alignment, only ribosomal marker genes, the top 5% of marker genes according to  $\Delta$ LL and the top 5% of marker genes further trimmed under default settings in BMGE 1.12 (Criscuolo and Gribaldo, 2010). Divergence time analyses were performed in MCMCTree (Yang, 2007) under a strict clock model. We used the normal approximation approach, with branch lengths estimated in codeml under the LG+G4 model. In each case, a fixed tree topology was used alongside a single calibration on the Cyanobacteria-Melainabacteria split. The calibration was modelled as a uniform prior distribution between 2.5 and 2.6 Ga, with a 2.5% probability that either bound could be exceeded. For each alignment, four independent MCMC chains were run for 2,000,000 generations to achieve convergence.

# *Plotting*

Statistical analyses were performed using R 4.0.4 (R Core Team, 2021), and data were plotted with ggplot2 (Wickham, 2016).

## Data and code availability

All of the data, including sequence alignments, trees, annotation files, and scripts associated with this manuscript have been deposited in the FigShare repository at DOI: 10.6084/m9.figshare.13395470.

## Acknowledgements

ERRM was supported by a Royal Society Enhancement Award (RGF\EA\180199) to TAW. CP was supported by NERC grant NE/P00251X/1 to TAW. This work was funded by the Gordon and Betty Moore Foundation through grant GBMF9741 to TAW, AS and GJSz. TAW was supported by a Royal Society University Research Fellowship (URF\R\201024). GJSz received funding from the European Research Council under the European Union's Horizon 2020 research and innovation program under Grant Agreement 714774 and Grant GINOP-2.3.2.-15-2016- 00057. AS is supported by the Swedish Research Council (VR starting grant 2016-03559), the NWO-I foundation of the Netherlands Organisation for Scientific Research (WISE fellowship) and the European Research Council (ERC Starting grant 947317, ASymbEL).

619

## 620 References

621

- 622 Adam PS, Borrel G, Brochier-Armanet C, Gribaldo S. 2017. The growing tree of Archaea:  
623 new perspectives on their diversity, evolution and ecology. *ISME J* **11**:2407–2425.
- 624 Altschul SF, Madden TL, Schäffer AA, Zhang J, Zhang Z, Miller W, Lipman DJ. 1997.  
625 Gapped BLAST and PSI-BLAST: a new generation of protein database search  
626 programs. *Nucleic Acids Research* **25**:3389–3402.
- 627 Aouad M, Borrel G, Brochier-Armanet C, Gribaldo S. 2019. Evolutionary placement of  
628 Methanonatronarchaeia. *Nature Microbiology* **4**:558–559.
- 629 Aramaki T, Blanc-Mathieu R, Endo H, Ohkubo K, Kanehisa M, Goto S, Ogata H. 2020.  
630 KofamKOALA: KEGG Ortholog assignment based on profile HMM and adaptive score  
631 threshold. *Bioinformatics* **36**:2251–2252.
- 632 Barboni M, Boehnke P, Keller B, Kohl IE, Schoene B, Young ED, McKeegan KD. 2017. Early  
633 formation of the Moon 4.51 billion years ago. *Science Advances* **3**:e1602365.
- 634 Bateman A, Coin L, Durbin R, Finn RD, Hollich V, Griffiths-Jones S, Khanna A, Marshall M,  
635 Moxon S, Sonnhammer ELL, Studholme DJ, Yeats C, Eddy SR. 2004. The Pfam protein  
636 families database. *Nucleic Acids Research* **32**:D138–41.
- 637 Betts HC, Puttick MN, Clark JW, Williams TA, Donoghue PCJ, Pisani D. 2018. Integrated  
638 genomic and fossil evidence illuminates life's early evolution and eukaryote origin.  
639 *Nature Ecology and Evolution* **2**:1556–1562.
- 640 Brown CT, Hug LA, Thomas BC, Sharon I, Castelle CJ, Singh A, Wilkins MJ, Wrighton KC,  
641 Williams KH, Banfield JF. 2015. Unusual biology across a group comprising more than  
642 15% of domain Bacteria. *Nature* **523**:208–211.
- 643 Buchfink B, Xie C, Huson DH. 2015. Fast and sensitive protein alignment using DIAMOND.  
644 *Nat Methods* **12**:59–60.
- 645 Cantarel BL, Coutinho PM, Rancurel C, Bernard T, Lombard V, Henrissat B. 2009. The  
646 Carbohydrate-Active EnZymes database (CAZy): an expert resource for  
647 Glycogenomics. *Nucleic Acids Research* **37**:D233–8.
- 648 Castelle CJ, Banfield JF. 2018. Major New Microbial Groups Expand Diversity and Alter our  
649 Understanding of the Tree of Life. *Cell* **172**:1181–1197.
- 650 Ciccarelli FD, Doerks T, von Mering C, Creevey CJ, Snel B, Bork P. 2006. Toward automatic  
651 reconstruction of a highly resolved tree of life. *Science* **311**:1283–1287.
- 652 Coleman GA, Davin AA, Mahendrarajah T, Spang A, Hugenholtz P, Szöllösi GJ, Williams  
653 TA. 2021. A rooted phylogeny resolves early bacterial evolution. *Science* **372**.  
654 doi:10.1126/science.abe5011
- 655 Cox CJ, Foster PG, Hirt RP, Harris SR, Embley TM. 2008. The archaeobacterial origin of  
656 eukaryotes. *Proceedings of the National Academy of Sciences of the United States of*  
657 *America* **105**:20356–20361.
- 658 Creevey CJ, Doerks T, Fitzpatrick DA, Raes J, Bork P. 2011. Universally distributed single-  
659 copy genes indicate a constant rate of horizontal transfer. *PLoS One* **6**:e22099.
- 660 Criscuolo A, Gribaldo S. 2010. BMGE (Block Mapping and Gathering with Entropy): a new  
661 software for selection of phylogenetic informative regions from multiple sequence  
662 alignments. *BMC Evolutionary Biology* **10**:210.
- 663 Da Cunha V, Gaia M, Gadelle D, Nasir A, Forterre P. 2017. Lokiarchaea are close relatives  
664 of Euryarchaeota, not bridging the gap between prokaryotes and eukaryotes. *PLoS*  
665 *Genetics* **13**:e1006810.
- 666 Dagan T, Roettger M, Bryant D, Martin W. 2010. Genome networks root the tree of life  
667 between prokaryotic domains. *Genome Biology and Evolution* **2**:379–392.
- 668 Dombrowski N, Williams TA, Sun J, Woodcroft BJ, Lee J-H, Minh BQ, Rinke C, Spang A.



2020. Undinarchaeota illuminate DPANN phylogeny and the impact of gene transfer on  
archaeal evolution. *Nature Communications* **11**:1–15.
- Finn RD, Clements J, Eddy SR. 2011. HMMER web server: interactive sequence similarity  
searching. *Nucleic Acids Research* **39**:W29–W37.
- Foster PG. 2004. Modeling compositional heterogeneity. *Systematic Biology* **53**:485–495.
- Fournier GP, Gogarten JP. 2010. Rooting the ribosomal tree of life. *Molecular Biology and  
Evolution* **27**:1792–1801.
- Galperin MY, Kristensen DM, Makarova KS, Wolf YI, Koonin EV. 2019. Microbial genome  
analysis: the COG approach. *Briefings in Bioinformatics* **20**:1063–1070.
- Gogarten JP, Kibak H, Dittrich P, Taiz L, Bowman EJ, Bowman BJ, Manolson MF, Poole RJ,  
Date T, Oshima T, Konishi J, Denda K, Yoshida M. 1989. Evolution of the vacuolar H<sup>+</sup>-  
ATPase: implications for the origin of eukaryotes. *Proceedings of the National Academy  
of Sciences of the United States of America* **86**:6661–6665.
- Gouy R, Baurain D, Philippe H. 2015. Rooting the tree of life: the phylogenetic jury is still out.  
*Philosophical Transactions of the Royal Society B Biological Sciences* **370**:20140329.
- Guy L, Ettema TJG. 2011. The archaeal “TACK” superphylum and the origin of eukaryotes.  
*Trends in Microbiology* **19**:580–587.
- Haft DH, Selengut JD, White O. 2003. The TIGRFAMs database of protein families. *Nucleic  
Acids Research* **31**:371–373.
- Hanan BB, Tilton GR. 1987. 60025: relict of primitive lunar crust? *Earth and Planetary  
Science Letters* **84**:15–21.
- Harris JK, Kelley ST, Spiegelman GB, Pace NR. 2003. The genetic core of the universal  
ancestor. *Genome Research* **13**:407–412.
- Hoang DT, Chernomor O, von Haeseler A, Minh BQ, Vinh LS. 2018. UFBoot2: Improving the  
Ultrafast Bootstrap Approximation. *Molecular Biology and Evolution* **35**:518–522.
- Horita J, Berndt ME. 1999. Abiogenic methane formation and isotopic fractionation under  
hydrothermal conditions. *Science* **285**:1055–1057.
- Hug LA, Baker BJ, Anantharaman K, Brown CT, Probst AJ, Castelle CJ, Butterfield CN,  
Hernsdorf AW, Amano Y, Ise K, Suzuki Y, Dudek N, Relman DA, Finstad KM,  
Amundson R, Thomas BC, Banfield JF. 2016. A new view of the tree of life. *Nature  
Microbiology* **1**:16048 doi:10.1038/nmicrobiol.2016.48
- Iwabe N, Kuma K, Hasegawa M, Osawa S, Miyata T. 1989. Evolutionary relationship of  
archaeobacteria, eubacteria, and eukaryotes inferred from phylogenetic trees of  
duplicated genes. *Proceedings of the National Academy of Sciences of the United  
States of America* **86**:9355–9359.
- Jeffroy O, Brinkmann H, Delsuc F, Philippe H. 2006. Phylogenomics: the beginning of  
incongruence? *Trends in Genetics* **22**:225–231.
- Jones P, Binns D, Chang H-Y, Fraser M, Li W, McAnulla C, McWilliam H, Maslen J, Mitchell  
A, Nuka G, Pesseat S, Quinn AF, Sangrador-Vegas A, Scheremetjew M, Yong S-Y,  
Lopez R, Hunter S. 2014. InterProScan 5: genome-scale protein function classification.  
*Bioinformatics* **30**:1236–1240.
- Kalyaanamoorthy S, Minh BQ, Wong TKF, von Haeseler A, Jermini LS. 2017. ModelFinder:  
fast model selection for accurate phylogenetic estimates. *Nature Methods* **14**:587–589.
- Katoh K, Standley DM. 2013. MAFFT multiple sequence alignment software version 7:  
improvements in performance and usability. *Molecular Biology and Evolution* **30**:772–  
780.
- Katoh K, Toh H. 2008. Recent developments in the MAFFT multiple sequence alignment  
program. *Briefings in Bioinformatics*. **9**(4):286–298 doi:10.1093/bib/bbn013
- Lartillot N, Brinkmann H, Philippe H. 2007. Suppression of long-branch attraction artefacts in  
the animal phylogeny using a site-heterogeneous model. *BMC Evolutionary Biology*  
**7**:S4.
- Lartillot N, Philippe H. 2004. A Bayesian mixture model for across-site heterogeneities in the  
amino-acid replacement process. *Molecular Biology and Evolution* **21**:1095–1109.
- Lepland A, Arrhenius G, Cornell D. 2002. Apatite in early Archean Isua supracrustal rocks,  
southern West Greenland: its origin, association with graphite and potential as a



biomarker. *Precambrian Research* **118**:221–241.

Martijn J, Schön ME, Lind AE, Vosseberg J, Williams TA, Spang A, Ettema TJG. 2020. Hikarchaeia demonstrate an intermediate stage in the methanogen-to-halophile transition. *Nature Communications* **11**:5490.

Méheust R, Burstein D, Castelle CJ, Banfield JF. 2019. The distinction of CPR bacteria from other bacteria based on protein family content. *Nature Communications* **10**:4173.

Minh BQ, Schmidt HA, Chernomor O, Schrempf D, Woodhams MD, von Haeseler A, Lanfear R. 2020. IQ-TREE 2: New Models and Efficient Methods for Phylogenetic Inference in the Genomic Era. *Molecular Biology and Evolution* **37**:1530–1534.

Mirarab S, Reaz R, Bayzid MS, Zimmermann T, Swenson MS, Warnow T. 2014. ASTRAL: genome-scale coalescent-based species tree estimation. *Bioinformatics* **30**:i541–8.

Mukherjee S, Seshadri R, Varghese NJ, Eloe-Fadrosh EA, Meier-Kolthoff JP, Göker M, Coates RC, Hadjithomas M, Pavlopoulos GA, Paez-Espino D, Yoshikuni Y, Visel A, Whitman WB, Garrity GM, Eisen JA, Hugenholtz P, Pati A, Ivanova NN, Woyke T, Klenk H-P, Kyrpides NC. 2017. 1,003 reference genomes of bacterial and archaeal isolates expand coverage of the tree of life. *Nature Biotechnology* **35**:676–683.

Parks DH, Chuvochina M, Waite DW, Rinke C, Skarshewski A, Chaumeil P-A, Hugenholtz P. 2018. A standardized bacterial taxonomy based on genome phylogeny substantially revises the tree of life. *Nature Biotechnology* **36**: 996-1004. doi:10.1038/nbt.4229

Parks DH, Rinke C, Chuvochina M, Chaumeil P-A, Woodcroft BJ, Evans PN, Hugenholtz P, Tyson GW. 2017. Recovery of nearly 8,000 metagenome-assembled genomes substantially expands the tree of life. *Nature Microbiology* **2**:1533–1542.

Petitjean C, Deschamps P, López-García P, Moreira D. 2014. Rooting the domain archaea by phylogenomic analysis supports the foundation of the new kingdom Proteoarchaeota. *Genome Biology and Evolution* **7**:191–204.

Pühler G, Leffers H, Gropp F, Palm P, Klenk HP, Lottspeich F, Garrett RA, Zillig W. 1989. Archaeobacterial DNA-dependent RNA polymerases testify to the evolution of the eukaryotic nuclear genome. *Proceedings of the National Academy of Sciences of the United States of America* **86**:4569–4573.

Quang LS, Gascuel O, Lartillot N. 2008. Empirical profile mixture models for phylogenetic reconstruction. *Bioinformatics* **24**:2317–2323.

Ramulu HG, Groussin M, Talla E, Planel R, Daubin V, Brochier-Armanet C. 2014. Ribosomal proteins: toward a next generation standard for prokaryotic systematics? *Molecular Phylogenetics and Evolution* **75**:103–117.

Rawlings ND, Barrett AJ, Finn R. 2016. Twenty years of the MEROPS database of proteolytic enzymes, their substrates and inhibitors. *Nucleic Acids Research* **44**:D343–50.

Raymann K, Brochier-Armanet C, Gribaldo S. 2015. The two-domain tree of life is linked to a new root for the Archaea. *Proceedings of the National Academy of Sciences* **112**:6670–6675.

R Core Team. 2021. R: A language and environment for statistical computing. R Foundation for Statistical Computing, Vienna, Austria.

Saier MH Jr, Tran CV, Barabote RD. 2006. TCDB: the Transporter Classification Database for membrane transport protein analyses and information. *Nucleic Acids Research* **34**:D181–6.

Schrempf D, Lartillot N, Szöllösi G. 2020. Scalable empirical mixture models that account for across-site compositional heterogeneity. *Mol Biol Evol.* doi:10.1093/molbev/msaa145

Seemann T. 2014. Prokka: rapid prokaryotic genome annotation. *Bioinformatics* **30**:2068–2069.

Segata N, Börnigen D, Morgan XC, Huttenhower C. 2013. PhyloPhlAn is a new method for improved phylogenetic and taxonomic placement of microbes. *Nature Communications* **4**:2304.

Shimodaira H. 2002. An approximately unbiased test of phylogenetic tree selection. *Systematic Biology* **51**:492–508.

Søndergaard D, Pedersen CNS, Greening C. 2016. HydDB: A web tool for hydrogenase

classification and analysis. *Scientific Reports* **6**:34212.

Sorokin DY, Makarova KS, Abbas B, Ferrer M, Golyshin PN, Galinski EA, Ciordia S, Mena MC, Merkel AY, Wolf YI, van Loosdrecht MCM, Koonin EV. 2017. Discovery of extremely halophilic, methyl-reducing euryarchaea provides insights into the evolutionary origin of methanogenesis. *Nature Microbiology* **2**:17081.

Spang A, Saw JH, Jørgensen SL, Zaremba-Niedzwiedzka K, Martijn J, Lind AE, van Eijk R, Schleper C, Guy L, Ettema TJG. 2015. Complex archaea that bridge the gap between prokaryotes and eukaryotes. *Nature* **521**:173–179.

Sugitani K, Mimura K, Takeuchi M, Lepot K, Ito S. 2015. Early evolution of large microorganisms with cytological complexity revealed by microanalyses of 3.4 Ga organic-walled microfossils. *Geobiology* **13**:507–521.

Taib, N, Megrian D, Witwinowski J, Adam P, Poppleton D, Borrel G, Beloin C, Gribaldo S. 2020. Genome-wide analysis of the Firmicutes illuminates the diderm/monoderm transition. *Nature ecology & evolution*, **4**(12):1661-1672.

Tourasse NJ, Gouy M. 1999. Accounting for Evolutionary Rate Variation among Sequence Sites Consistently Changes Universal Phylogenies Deduced from rRNA and Protein-Coding Genes. *Molecular Phylogenetics and Evolution* **13**:159–168.

Valas RE, Bourne PE. 2011. The origin of a derived superkingdom: how a gram-positive bacterium crossed the desert to become an archaeon. *Biology Direct* **6**:16.

van Zuilen MA, Lepland A, Arrhenius G. 2002. Reassessing the evidence for the earliest traces of life. *Nature* **418**:627–630.

Wang H-C, Li K, Susko E, Roger AJ. 2008. A class frequency mixture model that adjusts for site-specific amino acid frequencies and improves inference of protein phylogeny. *BMC Evolutionary Biology* **8**:331.

Wang H-C, Minh BQ, Susko E, Roger AJ. 2018. Modeling Site Heterogeneity with Posterior Mean Site Frequency Profiles Accelerates Accurate Phylogenomic Estimation. *Systematic Biology* **67**:216–235.

Wickham H. 2016. ggplot2: Elegant graphics for data analysis. Springer-Verlag New York.

Williams T a., Foster PG, Nye TMW, Cox CJ, Embley TM. 2012. A congruent phylogenomic signal places eukaryotes within the Archaea. *Philosophical Transactions of the Royal Society B Biological Sciences* **279**:4870–4879.

Williams TA, Cox CJ, Foster PG, Szöllösi GJ, Embley TM. 2020. Phylogenomics provides robust support for a two-domains tree of life. *Nature Ecology and Evolution* **4**:138–147.

Williams TA, Schrepf D, Szöllösi GJ, Cox CJ, Foster PG, Embley TM. 2021. Inferring the deep past from molecular data. *Genome Biology and Evolution*. doi:10.1093/gbe/evab067

Williams TA, Szöllösi GJ, Spang A, Foster PG, Heaps SE, Boussau B, Ettema TJG, Embley TM. 2017. Integrative modeling of gene and genome evolution roots the archaeal tree of life. *Proceedings of the National Academy of Sciences of the United States of America* **114**:E4602–E4611.

Xavier JC, Gerhards RE, Wimmer JLE, Brueckner J, Tria FDK, Martin WF. 2021. The metabolic network of the last bacterial common ancestor. *Communications Biology* **4**:413. doi:10.1038/s42003-021-01918-4

Yang Z. 2007. PAML 4: phylogenetic analysis by maximum likelihood. *Molecular Biology and Evolution* **24**:1586–1591.

Zhu Q, Mai U, Pfeiffer W, Janssen S, Asnicar F, Sanders JG, Belda-Ferre P, Al-Ghalith GA, Kopylova E, McDonald D, Kosciółek T, Yin JB, Huang S, Salam N, Jiao J-Y, Wu Z, Xu ZZ, Cantrell K, Yang Y, Sayyari E, Rabiee M, Morton JT, Podell S, Knights D, Li W-J, Huttenhower C, Segata N, Smarr L, Mirarab S, Knight R. 2019. Phylogenomics of 10,575 genomes reveals evolutionary proximity between domains Bacteria and Archaea. *Nature Communications* **10**. doi:10.1038/s41467-019-13443-4